Astronomy Letters, Vol. 29, No. 3, 2003, pp. 175–187. Translated from Pis'ma v Astronomicheskiĭ Zhurnal, Vol. 29, No. 3, 2003, pp. 208–222.
Original Russian Text Copyright © 2003 by Kholtygin, Monin, Surkov, Fabrika.

Fast Line-Profile Variability in the Spectra of O Stars

A. F. Kholtygin[1]*, D. N. Monin[2], A. E. Surkov[2], and S. N. Fabrika[2]

[1] *Astronomical Institute, St. Petersburg State University, Universitetskiĭ pr. 28, Petrodvorets, 198904 Russia*

[2] *Special Astrophysical Observatory, Russian Academy of Sciences, Nizhni Arkhyz, Karachaĭ-Cherkessian Republic, 357147 Russia*

Received October 14, 2002

Abstract—A program of the search for and analysis of profile variability in the spectra of bright O supergiants with a time resolution of 5–30 min is described. Preliminary results of the spectroscopic observations of the stars λ Ori, α Cam, and 19 Cep with the 1-m Special Astrophysical Observatory telescope in 2001 are presented. Line-profile variability was detected in the spectra of all the stars studied; variability in the Hα and C III λ5696 Å lines in the spectrum of λ Ori has been found for the first time. The variability amplitude is 4–5% for 19 Cep and 1–2% for α Cam and λ Ori on time scales from several hours to 3 or 4 days, and the width of the variable features reaches 2 Å (100 km s^{-1}). We detected cyclical variations in the He II λ4686 and C III λ5696 line profiles in the spectrum of λ Ori on time scales of 1.3–1.6 days. Rapid profile variations on time scales of 3.5–7 h were found in the violet parts of the Hα and He I λ4715 line profiles in the spectrum of λ Ori A. © *2003 MAIK "Nauka/Interperiodica".*

Key words: *stars, variable and peculiar; hot stars; line-profile variability.*

INTRODUCTION

One of the most important problems in the physics of stars is the formation of a complex internal structure in the expanding atmospheres of early-type (WR, O, and B) stars, i.e., the stellar-wind formation mechanism. Ultraviolet (Kaper *et al.* 1997, 1999), visible (Kaufer *et al.* 1996; Kaper *et al.* 1997; Lépine and Moffat 1999; de Jong *et al.* 1999, 2001), and X-ray (Kahn *et al.* 2001) observations of these stars suggest that there are inhomogeneities of various sizes and densities in their atmospheres.

The line profiles for WR stars exhibit variable features (subpeaks) that shift from the line center toward the line wings. These are associated with compact structures (commonly called clouds) in the atmosphere. The individual subpeaks contain no more than 1–2% of the total energy emitted in the line and, according to Lépine *et al.* (1996) and Lépine and Moffat (1999), the subpeaks themselves are short-lived profile features. The subpeaks with the highest flux have widths up to 200–300 km s^{-1} and are traceable in the profiles up to one or two days, whereas the smallest detected subpeaks with widths of about 50 km s^{-1} are seen in the profiles for no more than one or two hours. Small cloudlets that form narrow subpeaks with widths of 10–40 km s^{-1} (Kholtygin 1995), which are undetectable in the line profiles with currently available stellar spectroscopy, are assumed to be also present in the atmospheres.

This pattern of profile variability can be interpreted in terms of the stochastic cloud atmospheric model suggested by Kholtygin *et al.* (2000) and Kudryashova and Kholtygin (2001). In this model, which is a generalization of the cloud atmospheric model for Wolf–Rayet stars (Antokhin *et al.* 1988, 1992), the expanding stellar atmosphere (envelope) is a set of dense, small-scale inhomogeneities (clouds) in a rarefied intercloud medium. The formation and destruction of clouds in the atmosphere is treated as a stochastic process. Using the cloud model allows us to calculate both the ionization and thermal atmospheric structures and the variable profiles of the lines that originate in the atmosphere (Antokhin *et al.* 1992; Kudryashova and Kholtygin 2001). The concept of the stochastic cloud model was used to develop a three-phase cloud atmospheric model for early-type stars (Kholtygin 2001; Kholtygin *et al.* 2002). In this model, it is assumed that an ensemble of hot ($T = 10^6$–10^7 K) clouds that produce stellar X-ray radiation and of cold clouds in which ions of relatively low ionization stages (He II, C II, N II, and others) are preserved can be separated from the complete set of clouds.

The pattern of line-profile variability in the spectra of O and B stars is much more complex. Its clearest manifestation is the appearance of variable absorption features called discrete absorption components

* E-mail: afk@theor1.astro.spbu.ru

Table 1. A list of the program stars

HD	Name	Spectral type	V	V_∞	$V \sin i$, km s^{-1}	V_r, km s^{-1}
24212	ξ Per	O7.5III	4.04	2330	213	64.6
30614	α Cam	O9.5I	4.29	1590	129	6.1
36486	δ Ori	O9.5II	2.23	2060	144	118.3
36861	λ Ori A	O8III	3.66	2175	74	35.4
37742	ζ Ori A	O8III	1.79	1860	124	12.8
47839	15 Mon	O7Ve	4.66	2110	67	19.6
91316	ρ Leo	B1Iab	3.84	1110	75	42.0
203064	68 Cyg	O8e	5.04	2340	115	−3.9
209975	19 Cep	O9.5I	5.11	2010	95	−12.8
210839	λ Cep	O6Iab	5.09	2300	219	−75.9
214680	10 Lac	O9V	4.87	1140	35	−4.7

(DACs) in the profiles of the resonance and subordinate ultraviolet lines of N IV, Si IV, and other species. These features are detected in the violet parts of the profiles at frequencies that correspond to Doppler shifts from −300 to −800 km s^{-1} and then shift toward higher negative velocities until they reach the profile edge that corresponds to terminal wind velocities (1500–2500) km s^{-1}. The DAC formation is a cyclical process. The DAC evolution cycles are repeated at intervals of one or two days, while the overall pattern of DAC formation is stable over several years; the cycle length is virtually constant over the entire period of observations (de Jong *et al.* 1999), which argues for the hypothesis that the DAC formation is a periodic process.

The appearance of DACs is generally associated with the formation of large-scale structures in the stellar atmospheres in the regions where the star and the stellar wind corotate (Kaper *et al.* 1997; de Jong *et al.* 2001). The profile variability of the H I and He I lines in the visible spectrum of O stars is also associated with these structures. The fact that the periods of the optical-line profile variations are close to the DAC formation periods (Kaper *et al.* 1997) lends support to this hypothesis.

Although the line-profile variations in the spectra of early-type stars have long been studied, it is not yet completely clear why large-scale structures are formed. The presence of regions with different velocities and different mass outflow rates in the photospheres is suggested as one of the causes of their formation. The formation of such regions is associated with nonradial pulsations of O and B stars; the short-period (3–12 h) He I line profile variations detected in many B stars and six O stars (de Jong *et al.* 2001) serve as an indicator of these pulsations. One of the factors that favor the formation of large-scale atmospheric structures may be a weak (several hundred G) magnetic field on the stellar surface (Donati *et al.* 2001). However, as yet no evidence of a magnetic field has been found in O stars (Kaper *et al.* 1997).

Calculations of the dynamics of the expanding atmospheres in early-type stars (Owocki 1998) predict the radiative instability of the atmospheres of WR, O, and early-B stars and the formation of a broad spectrum of inhomogeneities in their atmospheres, both large-scale and small-scale ones. Because of the formation of small-scale inhomogeneities in the atmospheres, the optical line profiles in the spectra of all early-type stars must exhibit not only regular but also irregular (stochastic) profile variability characteristic of WR stars. This type of variability was found in the brightest O star ζ Pup. The subpeaks associated with small-scale inhomogeneities that shift toward the line wings were detected in the He II λ4686 Å line profiles in the spectrum of this star (Eversberg *et al.* 1998). No evidence of stochastic line-profile variability has yet been found in other O stars.

Note that the formation of large-scale structures in corotation regions is a stochastic process, as the shock front in the boundary region between fast and slow gaseous streams is unstable. This instability can lead to a breakup of the gaseous streams corotating with the star in its atmosphere into separate fragments. As a result, the line-profile variability in the stellar spectra will also be irregular.

For this reason, a detailed study of the regular and irregular (stochastic) line profile variability in the spectra of bright O stars attributable to the presence of small-scale inhomogeneities (clouds) in their atmospheres seems of current interest. This paper is the first in a series of papers that describe the results of such a study. We outline our program of searching for stochastic line-profile variability in the spectra of O stars and present the first results of our analysis of the line profiles for the stars α Cam, 19 Cep, and λ Ori obtained in 2001 with the 1-m Special Astrophysical Observatory (SAO) telescope.

THE PROGRAM OF SEARCHING FOR VARIABILITY

The studies of profile variability in early-type stars (Kaper *et al.* 1999; Eversberg *et al.* 1998; Kholtygin *et al.* 2000) indicate that high-quality spectroscopy is required to reliably detect both regular and stochastic profile variations: a spectral resolution of $R \geq 40\,000$; a signal-to-noise (S/N) ratio near the lines under

study of 200–300 or more; and a sufficiently high time resolution, 10–30 min.

Therefore, we selected bright ($V \leq 5^m.5$) northern-sky O stars whose spectra could be obtained with the parameters required to search for variability at the coudé focus using the CEGS coudè–echelle spectrograph of the 1-m SAO telescope (Musaev 1996). The program stars are listed in Table 1. Additionally, the list was supplemented with the bright B1 star ρ Leo to study the change in the pattern of profile variability when passing from late-O to early-B stars; during this passage, the mass-loss rate decreases sharply. The last columns of the table give terminal wind velocities V_∞ (Howarth *et al.* 1997), projected rotational velocities $V \sin i$ (Kaper *et al.* 1997), and radial velocities (Conti *et al.* 1977; Wilson 1953).

When choosing appropriate dates of observations, the program stars can be observed for almost the entire night. As a result, long series of observations (spanning two or three stellar rotation periods) needed for an accurate separation of the regular line-profile variability component can be obtained when they are observed for three to six nights. We suggest the following strategy for observations: obtaining long series of observations with the 1-m SAO telescope in order to reveal the overall pattern of variability in the program stars, and studying in detail those stars in which profile variability or any unusual spectral features were detected using the 6-m SAO telescope.

OBSERVATIONS OF THE PROGRAM STARS IN 2001

The first observations under the program described above were carried out during September 4–7 and November 29–December 4, 2001, with the 1-m SAO telescope. General data on these observations are given in Table 2.

The total number of spectra obtained in 2001 exceeds 200. Here, we consider the results of our observations for three stars: α Cam, 19 Cep, and λ Ori A. The results of our observations for the remaining program stars will be presented in the following publications. To achieve the signal-to-noise ratio S/N > 200 required to search for variability in the fainter star 19 Cep, we added the two spectra taken at adjacent times with 15-min-long exposures.

Organizing the Observations and Reducing the Spectroscopic Data

The program stars were observed with the CEGS coudé–echelle spectrograph of the 1-m SAO telescope. The configuration of this instrument was described by Musaev (1996). The detector was a Wright Instruments 1242 × 1152-pixel CCD array. With a spectrograph entrance slit width of 2″, the spectral resolution $R = 45\,000$ (0.08 Å pixel^{-1} near Hα) is achieved in the wavelength range from 4000 to 8000 Å.

Table 2. A list of the stars observed in 2001

Object	Exposure, min	Number of spectra	Total observing time, h
September 4–7, 2001			
ξ Per	10	4	0.7
α Cam	10	11	1.8
19 Cep	15	22	6.0
10 Lac	10–15	39	10.5
November 29–December 4, 2001			
ξ Per	5	5	0.4
α Cam	10	6	1.0
λ Ori A	10	75	12.5
ζ Ori A	2	36	1.2
10 Lac	15	27	6.7

The spectra were reduced by using the MIDAS package. The CCD image processing procedure included the following: scattered-light removal, echelle-order position determination, cosmic-ray particle hit removal, echelle-order extraction, continuum placement, correction for pixel-to-pixel CCD sensitivity nonuniformity, and spectrum linearization on the wavelength scale.

Since the operations described above were performed using standard procedures of the MIDAS package, we give comments only to those procedures that differ from the commonly used ones. The echelle spectra of the program stars were directly used to determine the order positions. We used the same order position mask for all the spectra of a given star taken on a given night.

To analyze the line-profile variability, we normalized the spectra to continuum. The continuum was placed separately in each echelle order by using a broad Gaussian-like filter (Shergin *et al.* 1996). For the entire sequence of spectra for a given star, we used the same parameters of the filter with a filter window width of 25–30 Å. In the three orders in the spectrum of λ Ori A with the Hα, C III λ5696 Å, and He II λ4686 Å lines, the continuum was placed by a different method: the spectrum was smoothed by a moving average, with the line regions being excluded from the procedure. We also studied the latter method

and tested it using spectroscopy for stars of various spectral types. It yields stable results in placing the continuum even if there are broad and variable lines in the spectrum or if the weather conditions change during the observations.

To make a correction for pixel-to-pixel CCD sensitivity nonuniformity, we observed the bright, rapidly rotating star α Leo ($V \sin i = 329$ km s^{-1}). As a result of this procedure, the S/N ratio in the individual spectrum increased by 20–50%, depending on the signal level and the residual pixel-to-pixel nonuniformities do not exceed 0.3% in amplitude.

The dispersion relation was derived from the spectrum of scattered solar light and its accuracy was 10 mÅ. Our reduction procedure ensures the same reduction of the entire sequence of spectra for a given star, which makes it possible to properly analyze the line-profile variability. For the wavelength calibration, we applied corrections for the Earth's rotation and its revolution around the Sun for each star.

Profile Variability

We elucidated the question of profile variability by using a standard technique. All spectra of the program star were added to obtain an average spectrum. The average Hβ and Hα profiles in the spectra of the program stars determined in this way are shown in Fig. 1. The radial velocities in Table 1 were used to transform the wavelength scale to the frame of reference associated with the star.

We determined the difference profiles (the individual profile minus the average profile) to identify variable features in the line profiles of all our spectra. Variable features were detected in the difference line profiles in the spectra of all our program stars. Figure 2 illustrates the difference Hα и He I λ5876 Å line profiles in the spectrum of 19 Cep, in units of the continuum intensity. The time axis is directed from the bottom upward. For clarity, the sequential profiles were displaced along the intensity scale. A variable feature with a maximum amplitude of 4–5% is clearly seen from the figure in the red part of the profile ($\approx$90 km s^{-1}). This feature shifted only slightly over the entire period of our observations of the star (6 h). Such variable features with the same velocity shift in the spectrum of this star were also detected in the Hβ profile.

Since the profile variation amplitude in the spectra of other program stars is appreciably smaller than that for 19 Cep, we used the following approach to ascertain whether the profile of a particular line was variable. For all wavelengths λ within the line profile, we calculated the quantity $\sigma_{\rm line}(\lambda)$—the standard deviation of the random variable $\Delta(\lambda, t)$, the difference between the individual and average line profiles for a given wavelength λ at time t. Simultaneously, we determined $\sigma_{\rm cont}$—a similar quantity for the continuum region near the line under consideration.

The measured flux in the difference spectrum at wavelength λ_j at time t_i can be represented as $F_j = F_j(t_i) = S_j + N_j$, where $S_j = S_j(t_i)$ is the sought-for signal and $N_j = N_j(t_i)$ is the noise component. Within one order, $N_j(t)$ can be assumed to be a normally distributed random variable with a zero mean and a variance $\sigma^2_{\rm cont}$. Let us analyze m difference spectra for the consecutive times $t_1, t_2, \ldots, t_m$. Assuming that the profiles are not variable ($N_j \gg S_j$), the random variable $S_{m-1} = \sigma_{\rm line}(\lambda)$ has the distribution $\sigma_{\rm cont}\sqrt{\chi^2/(m-1)}$, where χ^2 is the χ^2 distribution with $m-1$ degrees of freedom (see, e.g., Brandt 1975).

We specify a significance level α. Let the random variable

$$\sigma_{\rm line}(\lambda) > S^{\alpha}_{m-1}, \qquad (1)$$

where S^{α}_{m-1}, calculated for a given λ, is defined in such a way that the probability that this random variable exceeds $\sigma_{\rm line}(\lambda) > S^{\alpha}_{m-1}$ is equal to α. The hypothesis of a constant flux in the line at the significance level α is then rejected and the hypothesis of a variable component in the line is accepted.

The above procedure of searching for line-profile variability is similar to that used by Fullerton *et al.* (1996). These authors also used a procedure for smoothing the standard-deviation spectrum $\sigma_{\rm line}(\lambda)$ by taking into account the variation of the CCD sensitivity along the line profile. Since our technique for eliminating CCD sensitivity variations (pixel-to-pixel nonuniformity) proved to be efficient enough, no additional smoothing of the spectrum $\sigma_{\rm line}(\lambda)$ is required.

To illustrate our technique for searching variability, Fig. 3 shows the standard-deviation spectra $\sigma(\lambda)$ for the regions near the Hα, He II λ4686 Å, and C III λ5696 Å lines in the spectra of 19 Cep, α Cam, and λ Ori. We see from the figures that the lines in the spectra of all stars, except α Cam, satisfy the variability criterion (1). The position of the peak in the standard-deviation spectrum corresponds to the maximum line-profile variability amplitude. To increase the reliability of determining variable profiles in the spectra of the program stars, we used additional variability criteria based on the analysis of line-profile variations in the spectrum of a specific star:

(a) The lack of dependence of the profile variability pattern on the line position within a spectral order and the similarity of the profile variations for the same line

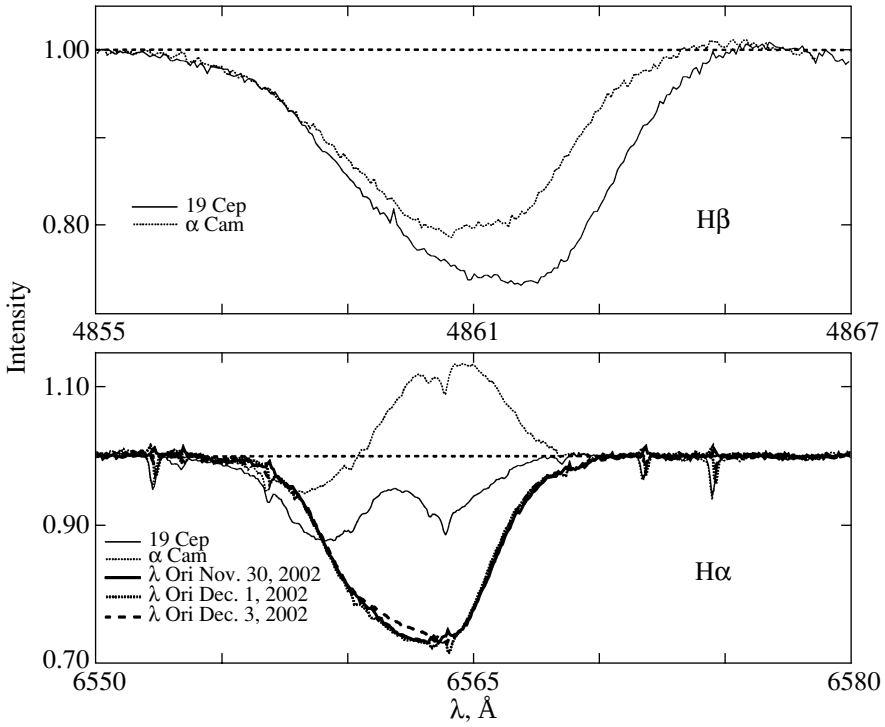

Fig. 1. Comparison of the Hα and Hβ profiles in the spectra of 19 Cep, α Cam, and λ Ori. The intensities (Y axis) are given in fractions of the continuum intensity.

in two adjacent orders (e.g., the Hβ and He I λ5876 Å lines);

(b) The same profile variability pattern for different lines of the same element and for lines of different elements (e.g., H, He, and C);

(c) Similar variability amplitudes for different lines; and

(d) Similar radial velocities of variable profile features for different lines.

Note, for example, that the variable features in the Hα and Hβ profiles in the spectrum of 19 Cep are shifted by 86 and 88 km s^{-1}, respectively.

An additional argument for the assumption that the profile variability we detected is real is that the variability was detected in the line profiles of the spectra of the stars under study, whereas in the profiles of intense unidentified interstellar bands (e.g., λ5778 and 5780 Å), no such variability was detected at a level down to 0.003 in flux units in the neighboring continuum. An additional argument for the reality of the profile variability is that the variability was detected in the profiles of strong H I, He I, He II, and C III lines, whereas no such variability was found in the profiles of intense unidentified interstellar bands (e.g. λ5778 and 5780 Å).

Table 3 gives a list of the lines for all of the program stars that satisfy criterion (1) with an allowance made for the above additional criteria (a)–(d). The profiles were found to be variable for all our program stars. At the same time, a variability of the Hα and C III λ5696 Å line profiles in the spectrum of λ Ori A has been detected for the first time (see Kaper *et al.* 1999). The similarity between the lists of variable lines for the program stars stems from the fact that the most intense lines in their spectra were included in the table. A significant increase in the signal-to-noise ratio is required to detect profile variability for weak lines.

The absence of lines that satisfy criterion (1) in the spectra of α Cam taken in September 2001 is attributable to the short period of our observations (less than 2 h) and to the small (11) number of spectra (see Table 2). At the same time, our observations of line profiles in the spectrum of this star in 1997 revealed variability of the He II λ4686 Å and Hα line profiles on time scales 2–4 h (Kholtygin *et al.* 2000).

The following technique is used to ascertain whether the line profiles are variable in the absence of their visible variations. Before obtaining the standard-deviation spectrum, the difference spectra are presmoothed by using a filter that is broad compared to the pixel size. In this case, if the filter width is $\Delta\lambda$ on the wavelength scale, then the amplitude of the random (noise) component of the difference profiles $\overline{N_j(t)}$ after applying the smoothing procedure

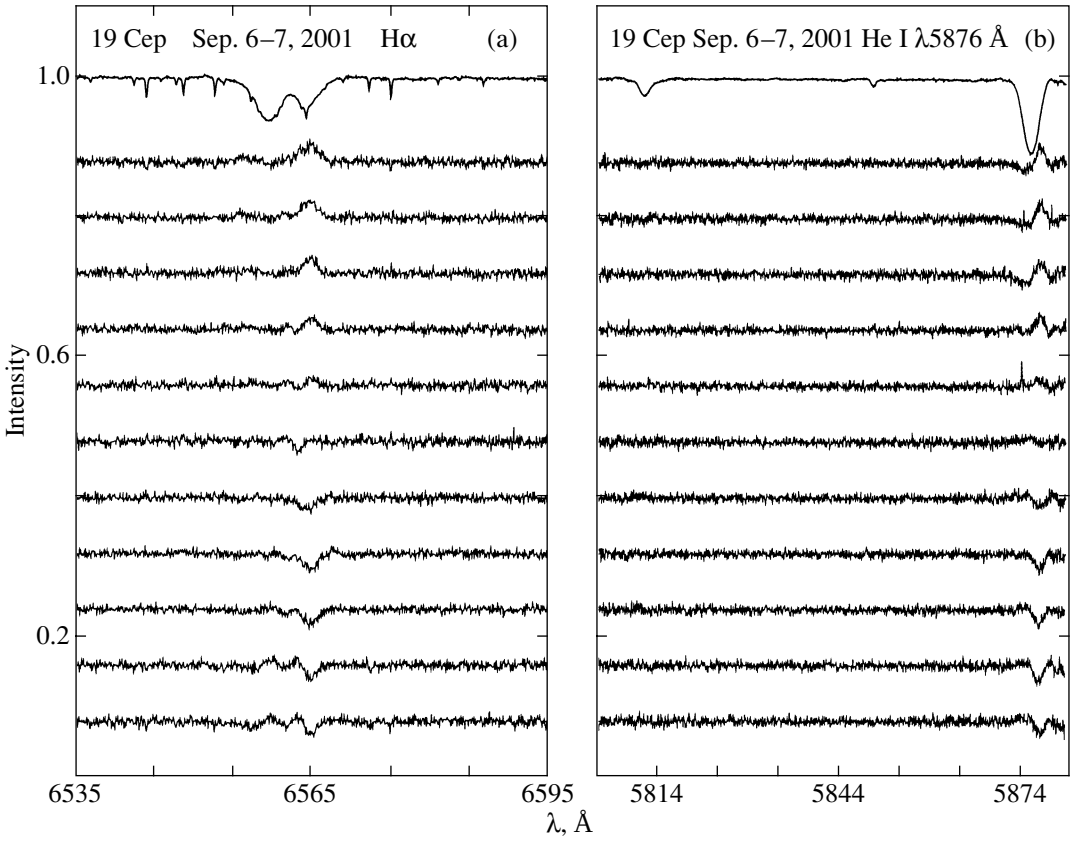

Fig. 2. Difference (a) Hα and (b) He I λ5876 Å line profiles in the spectrum of 19 Cep. The intensities are given in fractions of the continuum intensity. The individual profiles were displaced along the Y axis by 0.08 in the same units. The time axis is directed from the bottom upward. The upper curves are the mean profiles of the corresponding lines compressed by a factor of 2.5.

decreases by a factor of $\approx\sqrt{\Delta\lambda/\delta\lambda}$, where $\delta\lambda$ is the pixel width on the wavelength scale near the line under consideration. If the width of a variable component is not less than the filter width, then after applying the smoothing procedure, the peaks in the standard-deviation spectrum that correspond to the variable component are clearly distinguished. Figures 3b, 3d, 3f, and 3h illustrate the use of the profile smoothing procedure to analyze the profile variability.

It was empirically established that the most satisfactory results are obtained when smoothing the profiles with a Gaussian filter 0.5–1.0 Å (7–15 pixels) in width. An examination of Fig. 3 indicates that even if no significant profile variations are detected in the unsmoothed standard-deviation spectrum (Fig. 3c), presmoothing allows such variations to be distinguished quite clearly (see Fig. 3d). For several lines in the spectra of the program stars, criterion (1) is satisfied only for the smoothed difference spectra. A list of these lines is given in the last column of Table 3.

The question of how errors in the continuum placement affect the detection of profile variability should be considered separately. Analysis of these errors indicates that they increase with line width. However, even for the broadest lines, the absolute errors in continuum placement do not exceed 1%. In narrower lines, such as C III λ5696 Å or He II λ4686 Å, they are much smaller. In addition, the same procedure of continuum placement is used for all spectra. Thus, even the possible small errors in continuum placement affect all spectra in the same way.

The procedure of searching for profile variability described above only answers the question of whether the profile of a specific line is variable or not. At the same time, to elucidate the profile variability mechanism requires, as was noted in the Introduction, answering the question of whether the profile variations are to one or another degree regular (cyclical), irregular (stochastic), or a superposition of regular and irregular variations. To answer this question, it would be appropriate to use the techniques of Fourier (see, e.g., Roberts *et al.* 1987; Vityazev 2001) and wavelet (Dobeshi 2001; Kudryashova and Kholtygin 2001)

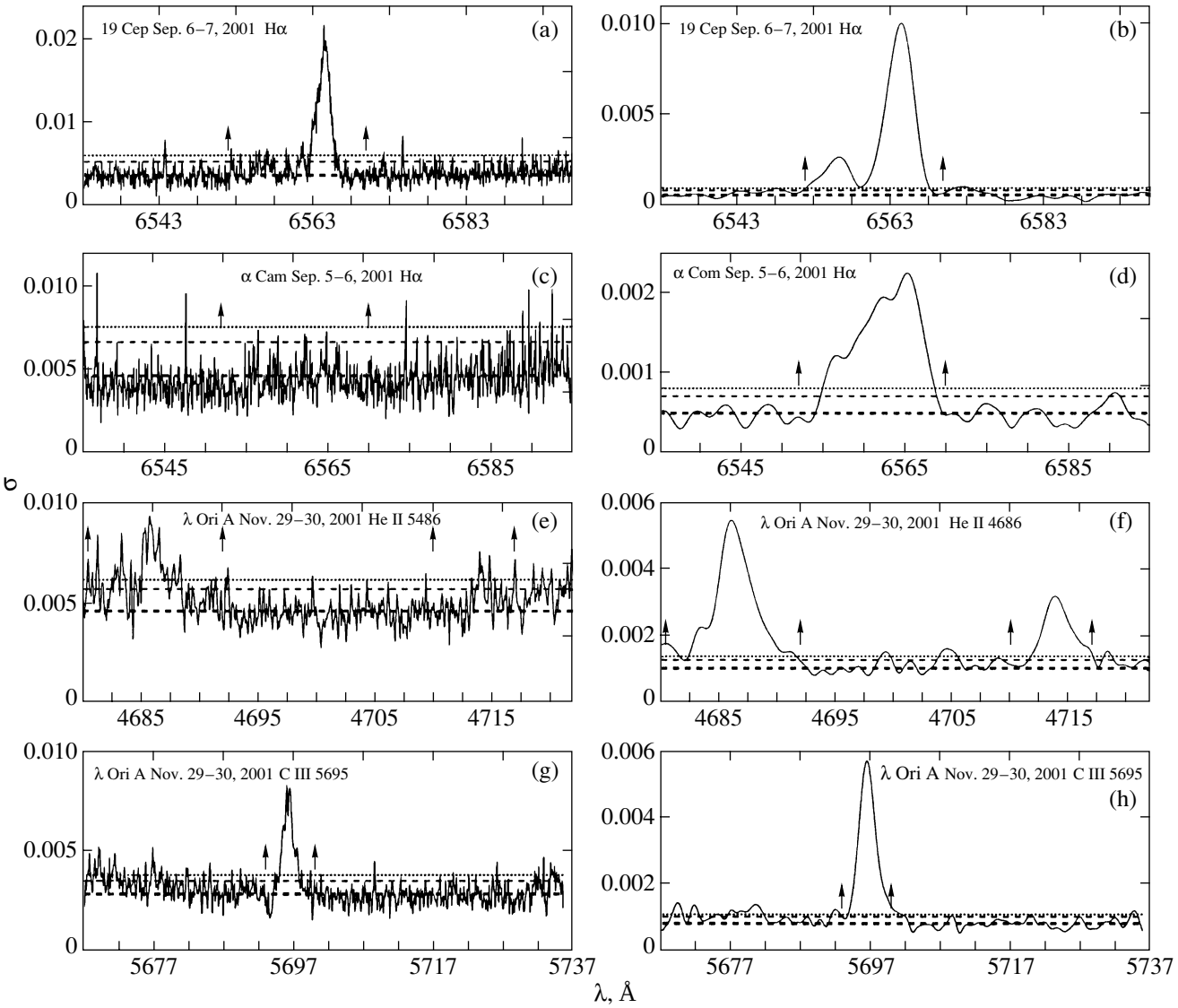

Fig. 3. Standard deviations of the difference Hα profiles in the spectra of 19 Cep, α Cam, and λ Ori A, in fractions of the continuum intensity. The horizontal lines in all figures correspond to the significance levels of the hypothesis that the profiles are not variable equal to 0.01, 0.05, and 0.50 (from the top downward). The arrows indicate the short- and long-wavelength boundaries of the line profiles. The unsmoothed and smoothed (with a 1.0-Å-wide Gaussian filter) difference line profiles were used in the left and right panels, respectively, to calculate the standard deviations.

analyses. The results of these analyses are described in the next sections.

VARIABILITY ANALYSIS

Wavelet Analysis

Analysis of the average line profiles in the spectra of the program stars (Fig. 1) and of the corresponding difference profiles (Fig. 2) indicates that the total line profile can be represented as a combination of the average profile and a large number of discrete features. The most suitable mathematical technique for studying the variability of such profiles is a wavelet analysis (see, e.g., Lépine *et al.* 1996). In this case, it would be appropriate to use the so-called MHAT wavelet $\psi(x) = (1 - x^2)\exp(-x^2/2)$ with a narrow power spectrum and zero zero and first moments as the analyzing (mother) wavelet. Note that the MHAT wavelet is the second derivative of the Gaussian function, which can be used to describe the shape of the features in the difference line profiles.

Using this wavelet, we can write the integral wavelet transform as (Lépine *et al.* 1996; Dobeshi

Table 3. Lines with variable profiles in the spectra of α Cam, 19 Cep, and λ Ori A

Star	Date of observation	Variable lines	Possible variability
19 Cep	Sep. 2001	Hβ, Hα, He I λ5876 Å	–
α Cam	Sep. 2001	–	He I λ4713 Å, Hβ, Hα
λ Ori A	Nov.–Dec. 2001	Hα, He II λ4686 Å, C III λ5696	He I λ4713 Å

2001):

$$W(s,u) = \frac{1}{s}\int\limits_{-\infty}^{\infty} f(x)\psi\left(\frac{x-u}{s}\right)dx \qquad (2)$$
$$= \int\limits_{-\infty}^{\infty} f(x)\psi_{su}(x)dx.$$

The signal power density $E_W(s,u) = W^2(s,u)$ characterizes the power distribution of the signal under study in space (s,u) = (scale, coordinate). Since in our case, the coordinate x is the wavelength, the scaling variable s can be expressed in Å.

The total power is distributed in scale in accordance with the global wavelet-transform power spectrum:

$$E_W(s) = \int\limits_{u_1}^{u_2} W^2(s,u)du = \int\limits_{u_1}^{u_2} E_W(s,u)du. \qquad (3)$$

The scale a where the function $E_W(s)$ reaches a maximum is called the dominant scale of the signal $f(x)$ under study on the interval u_1 and u_2 (Lépine *et al.* 1996).

We obtained wavelet power spectra for all the line profiles in the spectra of the programs stars in which variability was detected or suspected. The violet and red profile edges were used as u_1 and u_2, respectively. Thus, we considered the wavelet-transform power spectrum in the wavelength range that corresponded to the full profile width. Some of our spectra are shown in Fig. 4. Analysis of the power spectra reveals two components in the signal under study: small-scale (0.1–0.4 Å) and large-scale (0.5–8 Å) ones.

The first component in 19 Cep (Figs. 4a, 4b) and α Cam (Fig. 4c) changes only slightly over the period of our observations and has a maximum on a scale close to 0.1 Å, the CCD pixel size. The absence of noticeable variability of the small-scale component in the wavelet power spectrum for these stars provides evidence for the assumption that it is determined mainly by the noise contribution and by the residual effects of pixel-to-pixel CCD nonuniformity.

At the same time, the small-scale component in the wavelet power spectrum of the difference line profiles for λ Ori (Figs. 4d–4f) exhibits noticeable irregular variability with a maximum amplitude on the scale of 0.2–0.3 Å (10–15 km s^{-1}). The presence of a variable component in the wavelet power spectrum on these scales can be attributed to the existence of small-scale (10^{-3}–$10^{-2}R_\odot$) inhomogeneities in the atmosphere of λ Ori (Kudryashova and Kholtygin 2001).

The large-scale component in the wavelet power spectrum is highly variable for all our program stars. The maximum variability amplitude corresponds to the dominant scales of 1.5–6 Å, the characteristic size of variable features in the line profile (see Fig. 2). The time dependence of the power spectrum is the subject of the next section.

Periodic and Stochastic Line-Profile Variations

As was noted above, the studies of line profiles in the spectra of most O stars reveal their periodic variations. It would be natural to hypothesize that such variations also show up in the wavelet power spectrum of the difference line profiles. To test this hypothesis, we analyzed the time dependence of the integrated wavelet power spectra:

$$E[S_1,S_2](t) = \int\limits_{s_1}^{s_2} E_W(s,t)ds. \qquad (4)$$

Here, t is the time at which the profile under study was obtained, which is assumed to be equal to the midexposure time of the corresponding spectrum. The range 1.5–2.5 Å, in which the amplitude of the wavelet-spectrum variations is at a maximum, was chosen as the scale interval S_1, S_2. The derived functions $E[S_1,S_2](t)$ are plotted against the time of observation t in Figs. 4g–4l. For convenience, the time of observation is given in fractions of a day and the midexposure time of the first spectrum in the series of observations under study was taken to be zero.

As we see from Fig. 4, the dependences $E[S_1,S_2](t)$ are fairly regular. In searching for a harmonic component, we fitted the function $E[S_1,S_2](t)$ by a sine wave with the amplitude, period, phase, and shift determined by the least-squares method. The

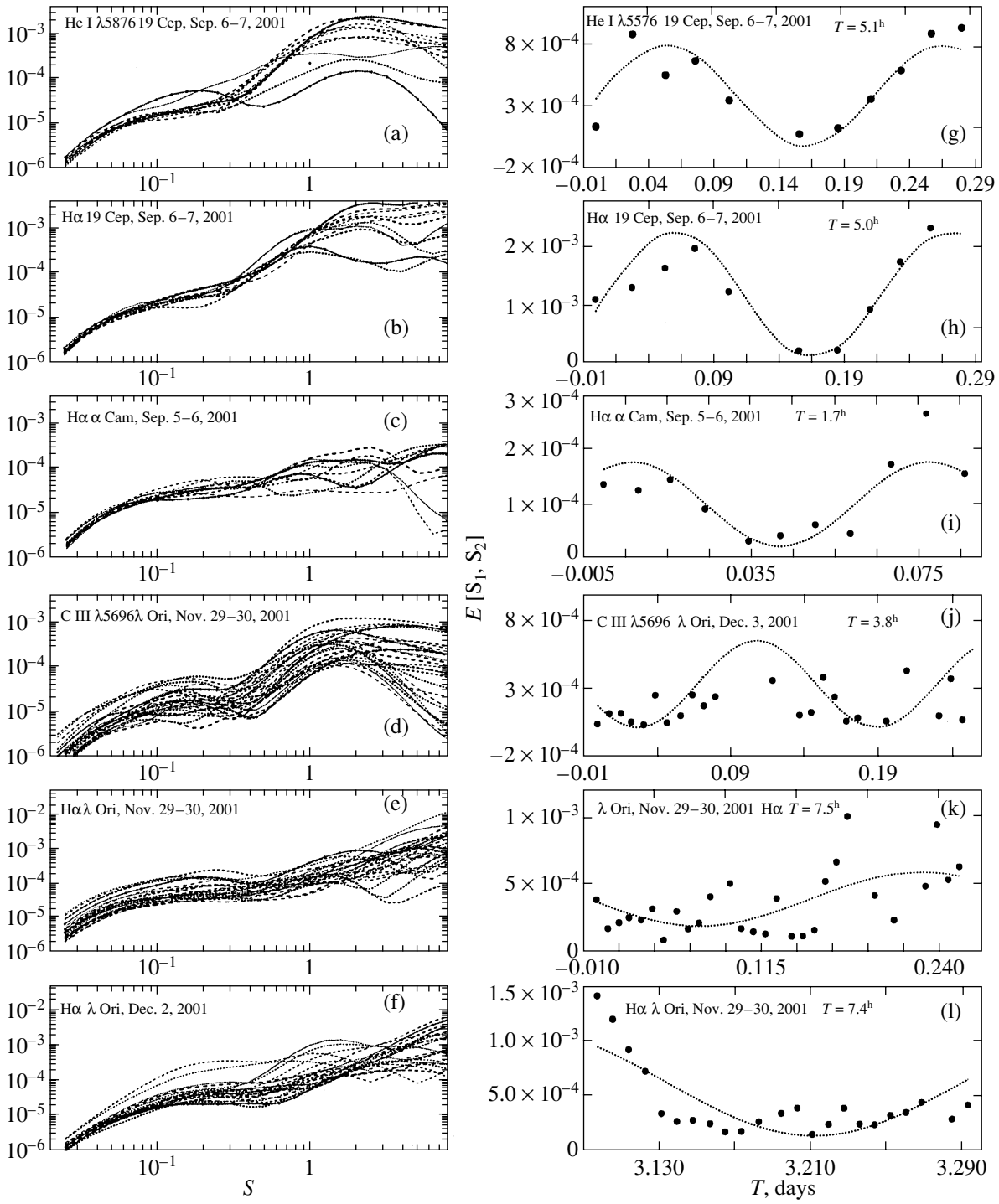

Fig. 4. (a–f) Wavelet power spectra of the difference profiles for the He I λ5876 Å, C III λ5696 Å, and Hα lines in the spectra of 19 Cep, α Cam, and λ Ori as a function of the wavelet-transform scale S in Å. (g–l) The total power-spectrum amplitudes in the scale range 1.5–2.5 Å (dots) versus the time of observation. The solid lines represent the sinusoidal fits.

derived fits are indicated in Figs. 4g–4l by the solid lines. Also shown in these figures are the inferred periods T of the wavelet power spectrum variations. The determined periods lie within the range $1.7–9.2^{\rm h}$ and correspond to the characteristic frequencies of the nonradial photospheric pulsations in stars of the corresponding spectral types (de Jong *et al.* 2001).

When the spectrum of λ Ori A was obtained, its companion λ Ori B ($5^{m}.61$) was within the spectrograph slit for about an hour out of the six hours

of observations (21–22 UT). For this reason, the question of how the companion contribution affects the line-profile variability is of considerable importance. The apparent magnitude of the companion is significantly fainter than that of the primary star (by $2^m.5$). In addition, no features were seen in the time dependence of the wavelet-transform amplitude (Figs. 4j–4l) when the companion was within the spectrograph slit. A detailed analysis revealed that the spectral scans across the dispersion were symmetric, suggesting that the line profiles are negligibly affected by the companion.

To elucidate the question of whether the periods found are real, we carried out a numerical experiment to determine the variation period of the function $E[S_1, S_2](t)$ from a model spectrum: a sinusoidal component plus a normally distributed noise component (N). As the times and the number of observed spectra (N_{sp}), we used the corresponding values for 19 Cep, α Cam, and λ Ori. The results of our experiment indicate that at the ratio A/N = 3–6, where A is the amplitude of the variable component and N is the noise level in the spectral range under consideration, with the number of spectra $k = 11$–30 and periods 1–10^h; the derived periods at a 0.95 confidence level lie in the interval $\pm 50\%$ of the original period of the harmonic component.

The effective value of A/N for the wavelet power spectra is determined by the S/N ratio for the original (nonnormalized) profiles of the program stars. It is A/N ≈ 6 for 19 Cep and α Cam and A/N ≈ 3 for λ Ori. Nevertheless, we believe that the conclusion regarding the detection of cyclical variations in the integrated wavelet power spectra would be premature. The time series shown in Figs. 4g–4l indicate that our derived periods are comparable to or even longer than the total period of observations of the program stars. Therefore, longer series of observations are required to confirm their reliability.

The period of the variations in the C III λ5696 Å emission line revealed by the analysis described above is approximately half the period of the variations in Hα, which may also suggest an insufficient reliability of the determined periods. It should be noted that the emission in these lines originate in different regions of the stellar atmosphere (Kaper *et al.* 1997). Therefore, the difference between the profile variation time scales may be quite real, although the question of whether the profile variations are periodic is still an open question.

Our analysis of the variations in the wavelet power spectrum is based on the assumption that one sinusoidal component mainly contributes to the variations in the function $E[S_1, S_2](t)$. More accurate methods should be used in the case of comparable contributions from harmonic components. For this reason, we performed a Fourier analysis of the line-profile variability in the spectrum of λ Ori A, for which the largest number (75) of profiles were obtained. All of the profiles observed over the three days of observations are difficult to use for our analysis, because there are long gaps (18 and 42 h) between the series of observations. These gaps result in a complex shape of the spectral window and require cleaning the Fourier spectrum from spurious peaks. To perform this procedure, we used the CLEAN algorithm (Roberts *et al.* 1987) in a modified version described by Vityazev (2001). To remove spurious components in the Fourier spectrum, we rejected all peaks at a confidence level lower than 0.99.

The square of the magnitude of the Fourier-transform amplitude (periodogram) for the time series $E[S_1, S_2](t)$ is shown for Hα in Fig. 5a. The periodogram exhibits only one peak at a frequency of 3.49 day^{-1}, which corresponds to a period of 6.9^h close to the period revealed by an elementary analysis (see Figs. 4k, 4l). Figure 5b illustrates the accuracy of fitting the time series by the harmonic component found.

It would be natural to assume that the frequencies of the periodic variations in the large-scale components of the line profiles must also be obtained when analyzing the variations in the profiles themselves. To test this assumption, we performed a Fourier analysis of the profile variations for the Hα, C III λ5696 Å, and He II λ4686 Å lines. The profile variations for each line were averaged over 25 km s^{-1} velocity intervals relative to the laboratory wavelengths of these lines.

To illustrate our results, Fig. 5c shows a Fourier spectrum of the temporal variations in the Hα profiles in the velocity range 25–50 km s^{-1}. In the figure, we see two close Fourier components with comparable amplitudes. Figure 5d shows the time dependence of the Hα profile deviations in this velocity range and their fit based on our Fourier analysis of the profiles. We see from the figure that the presence of two components with close frequencies in the Fourier spectrum can result in significant variations in the amplitude of the line-profile deviation from its average position in intervals of 1–3 days. Similar results are also obtained by analyzing the Hα profile in other velocity ranges. Note that the results of the Fourier analysis of the difference spectra and the wavelet power spectrum in Hα are similar.

At the same time, our Fourier analysis of the He I λ4714 Å, He II λ4686 Å, and C III λ5696 Å line profiles reveal a large set of frequencies in the Fourier spectra, those detected when analyzing Hα and other frequencies, as illustrated by Figs. 5e and 5g.

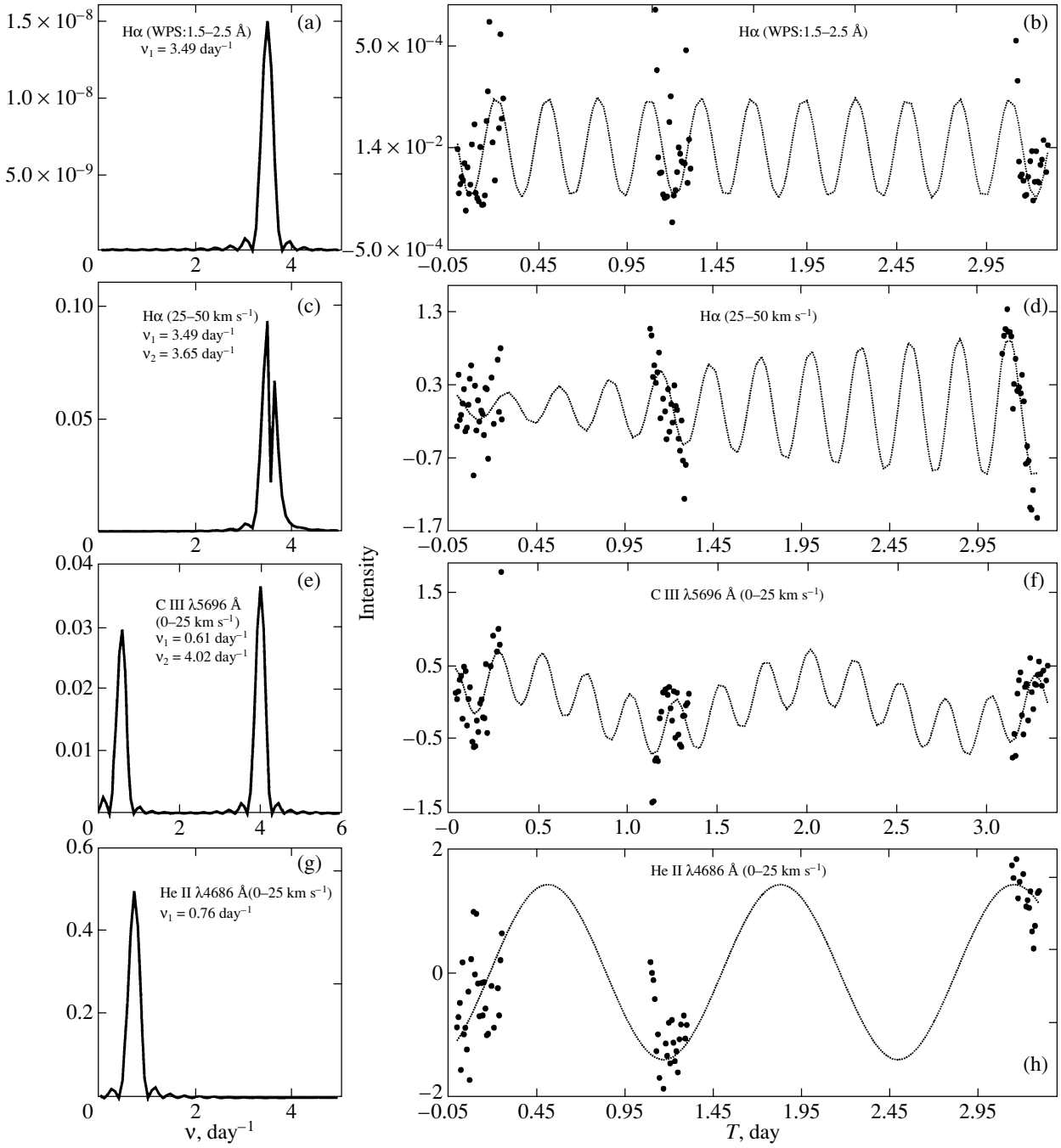

Fig. 5. (a) The periodogram of temporal variations in the wavelet power spectrum of the Hα line in the spectrum of λ Ori A in the range 1.5–2.5 Å determined from all of the spectra taken from November 30 through December 3, 2001; (b) a fit to the time dependence $E[S_1, S_2](t)$ for Hα; and (c) the same as (a) for the time dependence of the Hα profile deviations in the range 25–50 km s^{-1}. The continuum flux was assumed to be 100. (d) The same as (b) for the Hα profile variations; (e, f) the same as (c, d), for the C III λ5696 Å line ; and (g, h) the same as (c, d), for the He II λ4686 Å line.

Analysis of Line-Profile Variations

The Fourier analysis of the profile variations described in the preceding section shows the possible presence of both high-frequency and low-frequency components in the Fourier spectrum. The low-frequency components were detected in the profile variations for the He II λ4686 Å and C III λ5696 Å lines (see Figs. 5g, 5d); the frequencies of these components correspond to periods of $1^d.3$ and $1^d.6$, respectively. Kaper *et al.* (1997) detected profile

variation periods close to those found for λ Ori ($1-3^d$) in the Fourier spectra of the Hα profile variations in the spectra of the O stars O ξ Per, 68 Cyg, and λ Cep.

The regular profile variations for O stars with periods of several days are currently believed to be associated with the existence in their atmospheres of dense gaseous streams that corotate with the star at a distance of several tens of photospheric radii (Kaper *et al.* 1999; see, e.g., Fig. 21 in this paper). The profile variations are caused by the additional absorption of emission at line frequencies by the matter of the streams when they fall on the line of sight. Thus, the profile variation period is $P_n = P_{\rm rot}/n$, where $P_{\rm rot}$ is the stellar rotation period and n is the number of streams in the atmosphere.

The available data on profile variability in the spectrum of the star λ Ori itself are scarce. Its IUE ultraviolet observations (Kaper *et al.* 1999) reveal a DAC recurrence period in the Si IV $\lambda\lambda$1394, 1403 Å resonance line of $P_{\rm rec} = 5\overset{\rm d}{.}7$. Analysis of the variations in the difference profiles of the Si IV and N V $\lambda\lambda$1239, 11 243 Å resonance lines in the velocity range 1500–2000 km s^{-1} points to their regular variations with periods of $3\overset{\rm d}{.}4 \pm 0\overset{\rm d}{.}8$ and $4\overset{\rm d}{.}7 \pm 1\overset{\rm d}{.}4$, respectively. The above authors pointed out that the derived periods are unreliable because of the short period of observations and because of the detection of only one DAC event over the entire period of observation.

Thus, the presence of regular variations with periods $1\overset{\rm d}{.}3-1\overset{\rm d}{.}6$ in the spectrum of λ Ori can be said to be consistent with the available information on this star. Nevertheless, it would be premature to conclude that these periods were detected on the basis of our analysis of the profiles. According, for example, to Marchenko and Moffat (1998), when there are large gaps between the series of observations, even the choice of a high significance level does not give absolute confidence that the detected components in the Fourier spectrum are real. In light of these considerations, our detection of low-frequency components in the Fourier spectrum with periods $1\overset{\rm d}{.}3-1\overset{\rm d}{.}6$ needs to be additionally confirmed and the question of whether they are related to rotational profile modulation is still an open question.

Apart from the low-frequency components, the Fourier spectra of the profile variations for all the lines under study exhibit high-frequency components. The high-frequency components ($\nu = 2-8$ day^{-1}) are generally associated with nonradial photospheric pulsations (NRPs). The purely photospheric He I λ4713 Å line is considered to be the most convenient line for the detection of such components. Our analysis shows the possible presence of a component at frequency $\nu = 6.58$ day^{-1} ($P = 3.65^{\rm h}$) at the line center in the velocity range ($-25-100$ km s^{-1}) in the Fourier spectrum of the profile variations in this line in the spectrum of λ Ori. A $\nu = 4.39$ day^{-1} ($P = 5.47^{\rm h}$) component was detected in the violet part of the profile in the velocity range $-50 \ldots -25$ km s^{-1}. The same periods were found in the violet part of the He II λ4686 Å line profile.

In light of our remarks made above, we cannot assert that the presence of nonradial photospheric pulsations has been proven. To confirm this assertion and, if it is valid, to identify the periodic components found with specific (l, m) NRP modes requires a detailed analysis of the phase variations for these components along the line profiles (see, e.g., Schrijvers *et al.* 1997).

Apart from the components discussed above, we detected other components in the line-profile variations in the spectrum of λ Ori. In particular, the detection of short-period profile variations near the center of the C III emission line with the frequencies $\nu = 2.96$ day^{-1} ($P = 8.10^{\rm h}$) at $V =$ from -25 to 0 km s^{-1} and $\nu = 4.02$ day^{-1} ($P = 5.96^{\rm h}$) at $V = 0-25$ km s^{-1} (see Fig. 5e) proved to be unexpected.

A detailed analysis of these variations is to be performed in a separate publication. Note that the most reliable determination of the line profile periodicity pattern for the program stars requires obtaining their spectra with a high time resolution and with a much higher signal-to-noise ratio, which are to be taken with the 6-m SAO telescope in 2002. When using the 6-m telescope, a resolution of $R \approx 60\,000$ and a signal-to-noise ratio $S/N \approx 500-1000$ can be achieveed at short exposure times, up to 10–15 min.

CONCLUSIONS

We have presented our program of the search for and analysis of profile variability in the spectra of bright O supergiants with high time and spectral resolutions. Our observations and their analysis led us to the following conclusions.

(1) All of the program stars exhibit variable line profiles of hydrogen, He I and He II, C III, and other species. The variability amplitude is 4–5% for 19 Cep and 1–2% for α Cam and λ Ori on time scales of 6 h for 19 Cep and 1–3 days for λ Ori. The conclusion about profile variability is reliable at 0.99 confidence level.

(2) Variability of the Hα and C III λ5696 Å line profiles in the spectrum of λ Ori A was first detected at a 2% level of the continuum.

(3) The wavelet power spectra of the difference line profiles in the spectrum of λ Ori A were found to be variable on small scales: 0.2–0.3 Å (10–15 km s^{-1}), which may suggest the presence of small-scale perturbations in the stellar atmosphere.

(4) Our analysis of line profile variations is consistent with the hypothesis that regular profile variation components can exist. Low-frequency profile variations on time scales of 1.3–1.6 day consistent with the assumption of rotational profile modulation were detected in the variations of the He II λ4686 and C III λ5696 line profiles in the spectrum of λ Ori A.

(5) Short-period variations on time scales of 3.5–7 h close to the nonradial pulsation periods of O stars were detected in the violet parts of the Hα and He I λ4713 line profiles in the spectrum of λ Ori A.

ACKNOWLEDGMENTS

We are grateful to V.V. Vityazev for the remarks that improved the text of the paper and for providing the code that realizes the CLEAN algorithm. We are also grateful to A.B. Shneivais for help with the calculations. This study was supported by the Russian Foundation for Basic Research (project no. 01-02-16858) and the Federal Program "Research and Development in the Priority Fields of Science and Technology" (project "Studies of Energy Generation Mechanisms in Astrophysical Objects and the Behavior of Matter under Extreme Conditions ").

REFERENCES

1. I. I. Antokhin, A. F. Kholtygin, and A. M. Cherepashchuk, Astron. Zh. **65**, 558 (1988) [Sov. Astron. **32**, 285 (1988)].
2. I. I. Antokhin, T. Nugis, and A. M. Cherepashchuk, Astron. Zh. **69**, 516 (1992) [Sov. Astron. **36**, 260 (1992)].
3. Z. Brandt, *Statistical Methods of Monitoring Analysis* (Mir, Moscow, 1975), p. 87.
4. P. S. Conti, E. S. Leep, and J. J. Lorre, Astrophys. J. **214**, 759 (1977).
5. J. A. de Jong, H. F. Henrichs, S. Schrijvers, *et al.*, Astron. Astrophys. **345**, 172 (1999).
6. J. A. de Jong, H. F. Henrichs, L. Kaper, *et al.*, Astron. Astrophys. **368**, 601 (2001a).
7. J. A. de Jong, H. F. Henrichs, L. Kaper, *et al.*, Astron. Astrophys. **368**, 601 (2001b).
8. I. Dobeshi, *Ten Lections on Wavelets* (Moscow, 2001).
9. J.-F. Donati, G. A. Wade, J. Babel, *et al.*, Mon. Not. R. Astron. Soc. **326**, 1265 (2001).
10. T. Eversberg, S. Lépine, and A. F. J. Moffat, Astrophys. J. **494**, 799 (1998).
11. A. W. Fullerton, D. R. Gies, and C. T. Bolton, Astrophys. J., Suppl. Ser. **103**, 475 (1996).
12. I. D. Howarth, K. W. Siebert, G. A. J. Hussain, and R. K. Prinja, Mon. Not. R. Astron. Soc. **284**, 265 (1997).
13. S. M. Kahn, M. A. Leutenegger, J. Cottam, *et al.*, Astron. Astrophys. **365**, L312 (2001).
14. L. Kaper, H. F. Henrichs, A. W. Fullerton, *et al.*, Astron. Astrophys. **327**, 281 (1997).
15. L. Kaper, H. F. Henrichs, J. S. Nichols, *et al.*, Astron. Astrophys. **344**, 231 (1999).
16. A. Kaufer, O. Stahl, B. Wolf, *et al.*, Astron. Astrophys. **305**, 887 (1996).
17. A. F. Kholtygin, *Wolf-Rayet Stars: Binaries, Colliding Winds, Evolution, IAU Symp. 163,* Ed. by K. A. van DerHucht and P. M. Willams (Kluwer Acad. Publ., Dordrecht, 1995), p. 160.
18. A. F. Kholtygin, *All-Russian Astron. Conf., August 6–12, 2001* (St. Petersburg, 2001), p. 186.
19. A. F. Kholtygin, F. V. Kostenko, N. A. Kudryashova, and L. M. Oskinova, Astron. Soc. Pac. Conf. Ser. **204**, 227 (2000).
20. A. F. Kholtygin, J. C. Brown, J. P. Cassinelli, *et al.*, Astron. Astrophys. Trans. (2002) (in press).
21. N. A. Kudryashova and A. F. Kholtygin, Astron. Zh. **78**, 333 (2001) [Astron. Rep. **45**, 287 (2001)].
22. S. Lépine and A. F. J. Moffat, Astrophys. J. **514**, 909 (1999).
23. S. Lépine, A. F. J. Moffat, and R. N. Henriksen, Astrophys. J. **466**, 392 (1996).
24. S. Marchenko and A. F. J. Moffat, Astrophys. J. Lett. **499**, L195 (1998).
25. F. A. Musaev, Astron. Lett. **22**, 715 (1996).
26. S. P. Owocki, in *Proceedings of 2nd Guillermo Haro Conf.*, Ed. by J. Franco and A. Carraminana (Cambridge Univ. Press, Cambridge, 1998), p. 350.
27. D. H. Roberts, J. Lehar, and J. W. Dreher, Astron. J. **93**, 968 (1987).
28. C. Schrijvers, J. H. Telting, C. Aerts, *et al.*, Astron. Astrophys., Suppl. Ser. **121**, 343 (1997).
29. V. S. Shergin, A. Yu. Kniazev, and V. A. Lipovetsky, Astron. Nachr. **317**, 95 (1996).
30. V. V. Vityazev, *Analysis of Unevently Spaced Time Series* (Izd. St. Petersburg Gos. Univ., St. Petersburg, 2001).
31. R. F. Wilson, *III/21 General Catalogue of Stellar Radial Velocity* (Carnegie Institution of Washington, Washington D. C., 1953), Publ. 601.

Translated by V. Astakhov